PROBING GLUON SATURATION IN PHOTON+JET PRODUCTION IN pp AND pPb COLLISIONS*

Ishita Ganguli, Piotr Kotko

AGH University of Krakow
Faculty of Physics and Applied Computer Science
al. Mickiewicza 30, 30-059 Kraków, Poland

Received 24 March 2024, accepted 22 May 2024, published online 5 August 2024

We study photon+jet production in proton–proton and proton–lead collisions using the small-x Improved Transverse Momentum Dependent (ITMD) factorization framework in KaTie. The ITMD factorization framework, rooted in the Color Glass Condensate (CGC) theory (and for this particular process essentially identical to it), proves particularly useful at probing particle production at relatively large transverse momenta remaining at the same time sensitive to saturation effects in transverse momentum dependent (TMD) gluon distributions. Our investigation focuses on the azimuthal correlations and few other observables across a spectrum of center-of-mass energies. The comprehensive exploration of these observables leads to a deeper understanding of the underlying dynamics of gluons in the saturation domain.

DOI:10.5506/APhysPolBSupp.17.5-A36

1. Introduction

Gluon saturation is a fundamental phenomenon in Quantum Chromodynamics (QCD) that manifests at very high energies in hadronic collisions. As we move to these higher energies, the splitting of gluons gives rise to a power-like growth, but at some point during the evolution of the system, the growth is tamed due to gluon recombination. The gluons enter a collective state with transverse momenta of the order of a new emergent scale $Q_{\mathrm{s}}(x)$, where x is the Bjorken variable. Experimental studies, such as those conducted at the Relativistic Heavy Ion Collider (RHIC) and the Large Hadron

* Presented by I. Ganguli at the 30$^{\mathrm{th}}$ Cracow Epiphany Conference on *Precision Physics at High Energy Colliders*, Cracow, Poland, 8–12 January, 2024.

Collider (LHC), have already provided crucial insights into this phenomenon, from direct experimental data [1–3] to phenomenological studies based on HERA, RHIC, and LHC in [4–9]. Further studies of this densely packed regime is one of the main motivations for the future Electron–Ion Collider (EIC) [10], but even before that, there are opportunities to study saturation effects in the upcoming forward calorimeter (FoCal) at the LHC [11, 12].

The CGC framework [13–15] provides a universal description of many high-energy hadronic and nuclear processes and successfully describes the gluon dynamics at very high energies (small x). Our calculations here are based on the small-x Improved Transverse Momentum Dependent (ITMD) factorization framework [16]. In ITMD, forward production of particles is described via a set of TMD PDFs with corresponding off-shell gauge-invariant matrix elements.

The process we study here is

$$p(P_B) + A(P_A) \to \gamma(k_1) + J(k_2) + X\,, \tag{1}$$

where the A can either be a proton or a nucleus. In the very forward region it gives rise to a dilute-dense system where the target is probed at much smaller longitudinal momentum fractions x_A, as shown in Fig. 3.

The ITMD factorization formula for this kind of process was explicitly derived in [17] and is the same as the CGC formula [18]. At leading order for the dominant sub-process $g^*(k_A) + q(k_B) \to \gamma(k_1) + q(k_2)$, we have

$$\begin{aligned} \mathrm{d}\sigma_{pA\to j+\gamma} \;=\; & \int \mathrm{d}x_A\,\mathrm{d}x_B \int \mathrm{d}^2k_\mathrm{T}\, f_{q/B}(x_B;\mu)\, \mathcal{F}_{qg}^{(1)}\,(x_A, k_\mathrm{T};\mu) \\ & \times \mathrm{d}\sigma_{qg^*\to q\gamma}(x_A, x_B, k_\mathrm{T};\mu)\,, \end{aligned} \tag{2}$$

where $f_{q/B}$ is the collinear PDF, $\mathcal{F}_{qg}^{(1)}$ is essentially the dipole TMD PDF corresponding to target A. The incoming momenta are

$$k_A^\mu = x_A P_A^\mu + k_\mathrm{T}^\mu\,, \qquad k_B^\mu = x_B P_B^\mu\,, \tag{3}$$

with $k_\mathrm{T}\cdot P_A = k_\mathrm{T}\cdot P_B = 0$. For larger transverse momenta of radiated partons, effects of soft and collinear radiation become significant and Sudakov resummation has to be included, see the discussion in the original paper [19].

2. Results

In this section, we show numerical results for the photon and jet production. We use the proposed FoCal rapidity range of 3.8 to 5.1. The cross sections were calculated at three different center-of-mass energies for pp: 5 TeV, 8.8 TeV, and 14 TeV, while for pPb, only 8.8 TeV with three different transverse momentum thresholds ranging from 5 to 20 GeV. Within KaTie [20], the dipole gluon TMD was based on KS non-linear fit to HERA data [21], PDF was set to CT18NLO in LHAPDF [22].

Azimuthal correlations are sensitive to the transverse component present in the initial momenta and hence are key to observing saturation effects in the high-energy processes. In Fig. 1, we see the differential cross section as a function of azimuthal separation between the final states. The p–Pb cross section per nucleon shows clear signs of suppression as compared to p–p, especially in the back-to-back region and this suppression grows stronger as we move to lower p_{T} thresholds. This is best observed in the ratio of p–Pb differential cross section to p–p in Fig. 2

$$R_{p\mathrm{Pb}}^{\gamma+\mathrm{Jet}} = \frac{\left(\frac{\mathrm{d}\sigma}{\mathrm{d}\Delta\phi}\right)_{p\mathrm{Pb}}}{\left(\frac{\mathrm{d}\sigma}{\mathrm{d}\Delta\phi}\right)_{pp}} . \tag{4}$$

For the lowest p_{T} cut, we observe a $\sim 40\%$ suppression near $\Delta\varphi \sim \pi$ and for the highest p_{T} cut, this reduces to $\sim 20\%$. The theoretical uncertainty in both these cases were calculated by varying the hard scale by a factor of 2 and including the statistical errors in the Monte-Carlo generation. The plots in Fig. 3 are the differential cross sections in x_A and x_B, clearly showing $x_A \ll x_B$. This further justifies the use of the small-x ITMD framework.

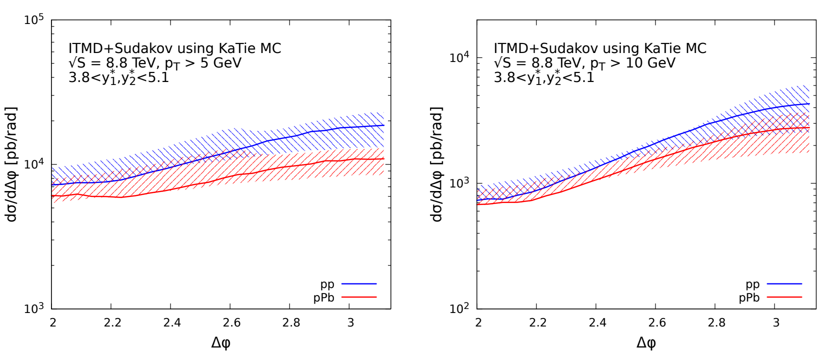

Fig. 1. Differential cross sections for γ+jet in FoCal acceptance range for p–p and p–Pb collisions at $\sqrt{s}$ = 8.8 TeV, as a function of azimuthal separation ($\Delta\varphi$). The three plots correspond to different transverse momentum cuts on final states: 5 GeV, 10 GeV, and 20 GeV.

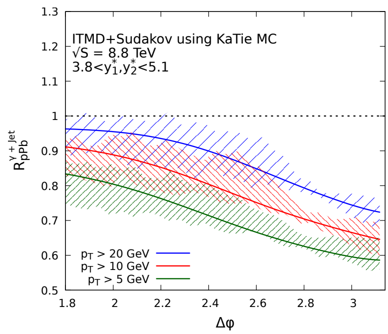

Fig. 2. Nuclear modification ratio as a function of the azimuthal angle difference $\Delta\varphi$ for γ+jet with three different p_{T} thresholds.

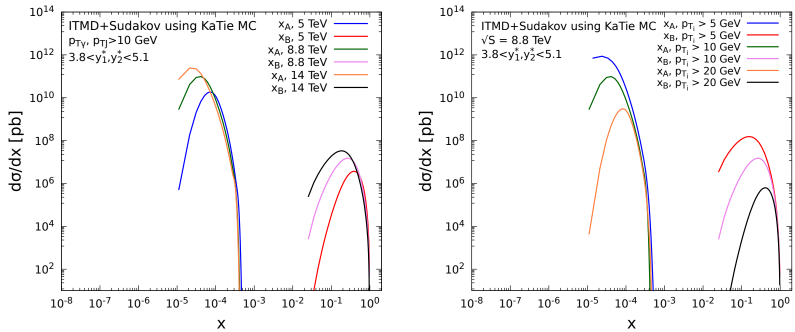

Fig. 3. Spectra of longitudinal fractions probed in the TMD PDF, x_A, and the collinear PDF, x_B for γ+jet production at different $\sqrt{s}$ energies in FoCal acceptance for moderate transverse momentum cut $p_{\mathrm{T}} > 10$ GeV (on the left), and at $\sqrt{s}$ energy 8.8 TeV in FoCal acceptance for different transverse momentum cut $p_{\mathrm{T}} > 5$ GeV, $p_{\mathrm{T}} > 10$ GeV, and $p_{\mathrm{T}} > 20$ GeV (on the right).

Finally, it is interesting to see how the p–p differential cross sections behave at different energies and under the influence of different evolution equations. Four different cases are shown in Fig. 4: ITMD with Sudakov resummation, ITMD without Sudakov resummation, linear version of KS TMD gluon distribution with Sudakov, and the running coupling BK (rcBK) equation [23, 24]. We observed a growing suppression in the large $\Delta\varphi$ region for moderate p_{T} cuts (both 10 and 20 GeV, except in the rcBK case). It was interesting to see that the trends for all p_{T} cuts were similar without the Sudakov resummation indicating a possibility of a non-trivial interplay between the shape of the curve and the cut-off, in the presence of the Sudakov resummation. The same calculations were also performed using the linear gluon distribution, which showed similar results. The trend is slightly different for the ratio of cross-sections with the rcBK gluon distribution, which might allow for the discrimination between models.

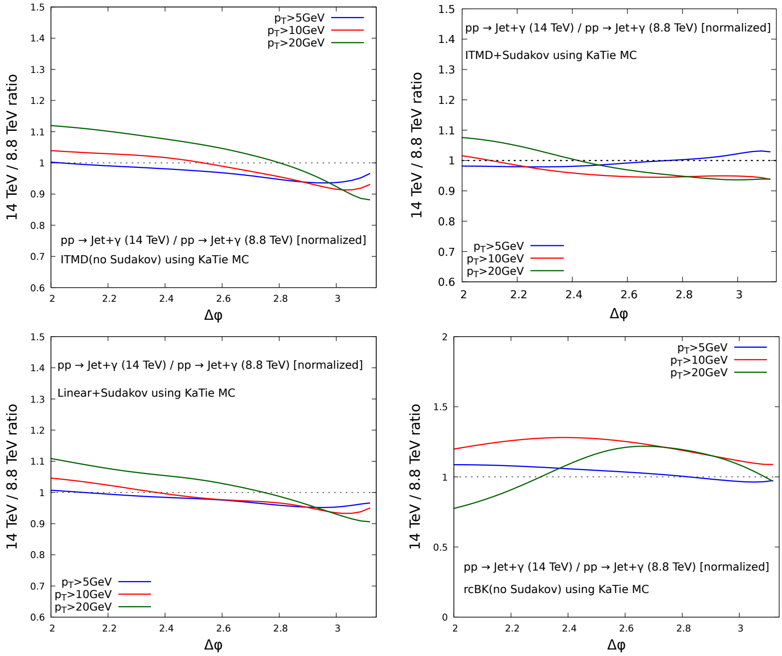

Fig. 4. Ratio of 14 TeV cross section to 8.8 TeV cross section, both independently normalized to the total cross section for γ+jet production in p–p collisions using — top left: ITMD without Sudakov resummation for different energies and transverse momentum cuts; top right: ITMD + Sudakov resummation; bottom left: linear gluon distributions with Sudakov resummation; and bottom right: running coupling BK gluon distribution.

3. Summary and outlook

We investigated azimuthal correlation, longitudinal momentum fraction along with some other observables (which were not shown here) for forward photon+jet production in p–p and p–Pb. The ITMD formulation can be rigorously derived from CGC for certain processes and for this particular process the ITMD factorization formula and the CGC result are essentially the same. The calculations were done within the FoCal kinematics. The results show strong signs of saturation effects and thus demonstrate the potential of the planned FoCal detector in studies of high-energy QCD.

I.G. and P.K. are supported by the National Science Centre (NCN), Poland grant No. 2020/39/O/ST2/03011.

REFERENCES

[1] STAR Collaboration (J. Adams *et al.*), *Phys. Rev. Lett.* **97**, 152302 (2006), arXiv:nucl-ex/0602011.

[2] PHENIX Collaboration (A. Adare *et al.*), *Phys. Rev. Lett.* **107**, 172301 (2011), arXiv:1105.5112 [nucl-ex].

[3] STAR Collaboration (M.S. Abdallah *et al.*), *Phys. Rev. Lett.* **129**, 092501 (2022), arXiv:2111.10396 [nucl-ex].

[4] K.J. Golec-Biernat, M. Wusthoff, *Phys. Rev. D* **59**, 014017 (1998), arXiv:hep-ph/9807513.

[5] T. Lappi, H. Mäntysaari, *Nucl. Phys. A* **908**, 51 (2013), arXiv:1209.2853 [hep-ph].

[6] J.L. Albacete, G. Giacalone, C. Marquet, M. Matas, *Phys. Rev. D* **99**, 014002 (2019), arXiv:1805.05711 [hep-ph].

[7] A. Stasto, S.-Y. Wei, B.-W. Xiao, F. Yuan, *Phys. Lett. B* **784**, 301 (2018), arXiv:1805.05712 [hep-ph].

[8] A. van Hameren, P. Kotko, K. Kutak, S. Sapeta, *Phys. Lett. B* **795**, 511 (2019), arXiv:1903.01361 [hep-ph].

[9] S. Benić, O. Garcia-Montero, A. Perkov, *Phys. Rev. D* **105**, 114052 (2022), arXiv:2203.01685 [hep-ph].

[10] A. Accardi *et al.*, *Eur. Phys. J. A* **52**, 268 (2016), arXiv:1212.1701 [nucl-ex].

[11] ALICE Collaboration, «Letter of Intent: A Forward Calorimeter (FoCal) in the ALICE experiment», tech. rep., CERN, Geneva, June 2020.

[12] ALICE Collaboration, «Physics of the ALICE Forward Calorimeter upgrade», 2023.

[13] F. Gelis, E. Iancu, J. Jalilian-Marian, R. Venugopalan, *Annu. Rev. Nucl. Part. Sci.* **60**, 463 (2010), arXiv:1002.0333 [hep-ph].

[14] Y.V. Kovchegov, E. Levin, «Quantum Chromodynamics at High Energy», in: «Quark–Gluon Plasma 3», *Cambridge University Press*, 2012.

[15] E. Iancu, R. Venugopalan, «The Color Glass Condensate and High Energy Scattering in QCD», *World Scientific*, 2004, pp. 249–363.

[16] P. Kotko *et al.*, *J. High Energy Phys.* **2015**, 106 (2015), arXiv:1503.03421 [hep-ph].

[17] T. Altinoluk, R. Boussarie, P. Kotko, *J. High Energy Phys.* **2019**, 156 (20219), arXiv:1901.01175 [hep-ph].

[18] F. Dominguez, C. Marquet, B.-W. Xiao, F. Yuan, *Phys. Rev. D* **83**, 105005 (2011), arXiv:1101.0715 [hep-ph].

[19] I. Ganguli, A. van Hameren, P. Kotko, K. Kutak, *Eur. Phys. J. C* **83**, 868 (2023).

[20] A. van Hameren, *Comput. Phys. Commun.* **224**, 371 (2018), arXiv:1611.00680 [hep-ph].

[21] K. Kutak, S. Sapeta, *Phys. Rev. D* **86**, 094043 (2012), arXiv:1205.5035 [hep-ph].

[22] A. Buckley *et al.*, *Eur. Phys. J. C* **75**, 132 (2015).

[23] J.L. Albacete *et al.*, *Eur. Phys. J. C* **71**, 1705 (2011), arXiv:1012.4408 [hep-ph].

[24] M. Hentschinski, K. Kutak, R. Straka, *Eur. Phys. J. C* **82**, 1147 (2022), arXiv:2207.09430 [hep-ph].